

DISCOVERY OF DRAMATIC OPTICAL VARIABILITY IN SDSS J1100+4421:
A PECULIAR RADIO-LOUD NARROW-LINE SEYFERT 1 GALAXY?

MASAO MI TANAKA¹, TOMOKI MOROKUMA², RYOSUKE ITOH³, HIROSHI AKITAYA⁴, NOZOMU TOMINAGA^{5,6}, YOSHIHIKO SAITO⁷, ŁUKASZ STAWARZ^{8,9}, YASUYUKI T. TANAKA⁴, POSHAK GANDHI¹⁰, GAMAL ALI¹¹, TSUTOMU AOKI¹², CARLOS CONTRERAS¹³, MAMORU DOI², AHMAD ESSAM¹¹, GAMAL HAMED¹¹, ERIC Y. HSIAO¹³, IKURU IWATA¹⁴, KOJI S. KAWABATA⁴, NOBUYUKI KAWAI⁷, YUKI KIKUCHI², NAOTO KOBAYASHI², DAISUKE KURODA¹⁵, HIROYUKI MAEHARA¹¹, EMIKO MATSUMOTO⁵, PAOLO A. MAZZALI^{16,17,18}, TAKEO MINEZAKI², HIROYUKI MITO¹¹, TAKASHI MIYATA², SATOSHI MIYAZAKI¹, KENSHO MORI³, YUKI MORITANI⁴, KANA MOROKUMA-MATSUI¹⁹, NIDIA MORRELL¹³, TOHRU NAGAO²⁰, YOSHIKAZU NAKADA², FUMIAKI NAKATA¹⁴, CHINAMI NOMA²¹, KEN OHSUGA¹, NORIO OKADA¹, MARK M. PHILLIPS¹³, ELENA PIAN^{22,23}, MICHAEL W. RICHMOND²⁴, DEVENDRA SAHU²⁵, SHIGEYUKI SAKO², YUKI SARUGAKU⁸, TAKUMI SHIBATA⁵, TAKAO SOYANO¹¹, MAXIMILIAN D. STRITZINGER²⁶, YUTARO TACHIBANA⁷, FRANCESCO TADDIA²⁷, KATSUTOSHI TAKAKI³, ALI TAKEY¹¹, KEN'ICHI TARUSAWA¹², TAKAHIRO U³, NOBUHARU UKITA¹⁵, YUJI URATA²⁸, EMMA S. WALKER²⁹, TAKETOSHI YOSHII⁷

Draft version September 5, 2014

ABSTRACT

We present our discovery of dramatic variability in SDSS J1100+4421 by the high-cadence transient survey Kiso Supernova Survey (KISS). The source brightened in the optical by at least a factor of three within about half a day. Spectroscopic observations suggest that this object is likely a narrow-line Seyfert 1 galaxy (NLS1) at $z = 0.840$, however with unusually strong narrow emission lines. The estimated black hole mass of $\sim 10^7 M_\odot$ implies bolometric nuclear luminosity close to the Eddington limit. SDSS J1100+4421 is also extremely radio-loud, with a radio loudness parameter of $R \simeq 4 \times 10^2 - 3 \times 10^3$, which implies the presence of relativistic jets. Rapid and large-amplitude optical variability of the target, reminiscent of that found in a few radio- and γ -ray loud NLS1s, is therefore produced most likely in a blazar-like core. The 1.4 GHz radio image of the source shows an extended structure with a linear size of about 100 kpc. If SDSS J1100+4421 is a genuine NLS1, as suggested here, this radio structure would then be the largest ever discovered in this type of active galaxies.

Subject headings: galaxies: active — galaxies: individual (SDSS J110006.07+442144.3) — galaxies: Seyfert — galaxies: jets

¹ National Astronomical Observatory of Japan, Mitaka, Tokyo 181-8588, Japan; masaomi.tanaka@nao.ac.jp

² Institute of Astronomy, School of Science, University of Tokyo, Mitaka, Tokyo 181-0015, Japan

³ Department of Physical Sciences, Hiroshima University, Higashi-Hiroshima, Hiroshima 739-8526, Japan

⁴ Hiroshima Astrophysical Science Center, Hiroshima University, Higashi-Hiroshima, Hiroshima 739-8526, Japan

⁵ Department of Physics, Faculty of Science and Engineering, Konan University, Kobe, Hyogo 658-8501, Japan

⁶ Kavli Institute for the Physics and Mathematics of the Universe (WPI), The University of Tokyo, Kashiwa, Chiba 277-8583, Japan

⁷ Department of Physics, Tokyo Institute of Technology, Meguro-ku, Tokyo 152-8551, Japan

⁸ Institute of Space and Astronautical Science, JAXA, Sagamihara, Kanagawa 252-5210, Japan

⁹ Astronomical Observatory, Jagiellonian University, ul. Orla 171, 30-244 Krakow, Poland

¹⁰ Department of Physics, Durham University, Durham DH1-3LE, UK

¹¹ National Research Institute of Astronomy and Geophysics, Helwan, Cairo, Egypt

¹² Kiso Observatory, Institute of Astronomy, School of Science, The University of Tokyo, Kiso, Nagano 397-0101, Japan

¹³ Carnegie Observatories, Las Campanas Observatory, Colina El Pino, Casilla 601, Chile

¹⁴ Subaru Telescope, National Astronomical Observatory of Japan, Hilo, HI 96720, USA

¹⁵ Okayama Astrophysical Observatory, National Astronomical Observatory of Japan, Asakuchi, Okayama 719-0232, Japan

¹⁶ Astrophysics Research Institute, Liverpool John Moores University, IC2, Liverpool Science Park, 146 Brownlow Hill, Liverpool L3 5RF, UK

¹⁷ Istituto Nazionale di Astrofisica-OAPd, vicolo dell'Osservatorio 5, I-35122 Padova, Italy

1. INTRODUCTION

It is widely accepted that active galactic nuclei (AGNs) are powered by supermassive black holes (BHs) accreting at high rates. Radio-loud AGNs are those which possess powerful relativistic jets. The radio loudness parameter R , i.e., the ratio of a radio flux to a nuclear optical flux of a source, is often used as a proxy for the jet pro-

¹⁸ Max-Planck-Institut für Astrophysik, Karl-Schwarzschild-Str. 1, D-85748 Garching, Germany

¹⁹ Nobeyama Radio Observatory, Nobeyama, Minamimaki, Minamisaku, Nagano 384-1305, Japan

²⁰ Research Center for Space and Cosmic Evolution, Ehime University, Bunkyo-cho, Matsuyama 790-8577, Japan

²¹ Astronomical Institute, Tohoku University, Aramaki, Aoba-ku, Sendai 980-8578, Japan

²² Scuola Normale Superiore di Pisa, Piazza dei Cavalieri 7, I-56126 Pisa, Italy

²³ INAF-Istituto di Astrofisica Spaziale e Fisica Cosmica, Via P. Gobetti 101, I-40129 Bologna, Italy

²⁴ Department of Physics, Rochester Institute of Technology, 85 Lomb Memorial Drive, Rochester, NY 14623-5603, USA

²⁵ Indian Institute of Astrophysics, Koramangala, Bangalore 560 034, India

²⁶ Department of Physics and Astronomy, Aarhus University, Ny Munkegade, DK-8000 Aarhus C, Denmark

²⁷ The Oskar Klein Centre, Department of Astronomy, Stockholm University, AlbaNova, SE-10691 Stockholm, Sweden

²⁸ Institute of Astronomy, National Central University, Chung-Li 32054, Taiwan

²⁹ Department of Physics, Yale University, New Haven, CT 06520-8120, USA

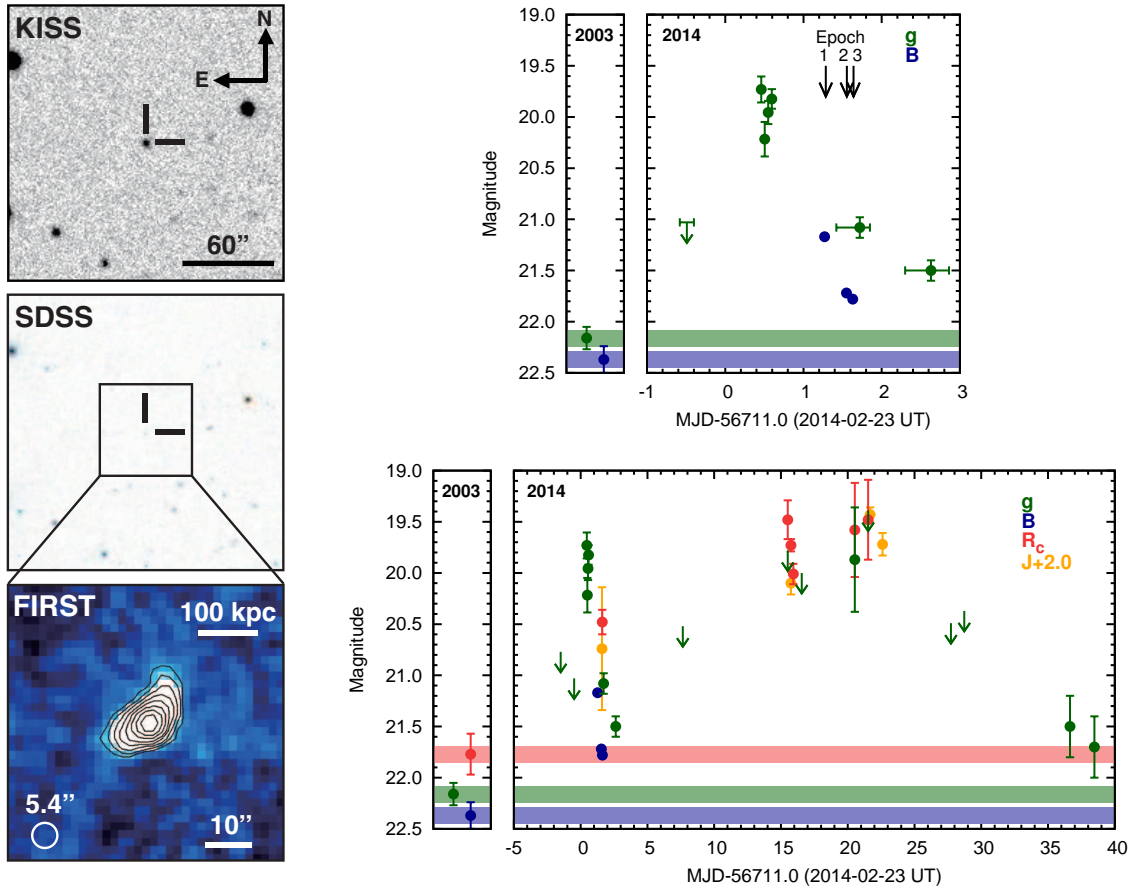


FIG. 1.— *Left*: Discovery image of SDSS J1100+4421 taken on 2014 Feb 23 UT with KWFC (upper), the SDSS image (middle), and the FIRST 1.4 GHz radio image (lower, the beam size is $5.4''$ as shown with the circle, White et al. 1997). The contour levels in the FIRST image start from 3σ ($1\sigma = 0.20$ mJy beam $^{-1}$), separated by a factor of $\sqrt{2}$. *Right*: Light curves of SDSS J1100+4421 around the discovery epoch (upper) and until 40 days after the flare (lower). The vertical arrows in black show the epochs of spectroscopic data. Our photometric data are compared with SDSS g -band magnitude and B - and R_c -band magnitudes estimated from SDSS magnitudes (left panel and shaded region). Magnitudes are given in the AB system for the SDSS g band and Vega units for the other bands.

duction efficiency. Several plausible relations between this parameter and other fundamental characteristics of a central engine (such as BH mass, accretion rate, and possibly BH spin) have been discussed in the literature (e.g., Sikora et al. 2007, and references therein). In general, AGNs with higher BH masses ($> 10^8 M_\odot$) and lower accretion rates tend to be more radio loud.

In this context, radio properties of NLS1s are of a particular interest, since AGNs of this peculiar type (Osterbrock & Pogge 1985; Pogge 2000) are believed to have relatively small BH masses ($10^6 - 10^8 M_\odot$) and very high accretion rates (e.g., Mathur 2000). By these properties, it had been inferred that NLS1s are a radio-quiet class of AGNs, and that young BHs in NLS1s that undergo rapid growth via high-rate accretion do not produce relativistic jets.

Statistical studies (e.g., Komossa et al. 2006; Whalen et al. 2006; Zhou et al. 2006 hereafter Z06) show, in fact, that the fraction of radio-loud NLS1s is small, i.e., only 7% of NLS1s have $R > 10$ while about 20 % of broad-line Seyfert 1 galaxies have $R > 10$ (Komossa et al. 2006). However, they also find that a small fraction ($\sim 2.5\%$) of NLS1s is very radio-loud ($R > 100$). Recently more and more radio-loud

NLS1s are being discovered (e.g., Yuan et al. 2008; Caccianiga et al. 2014). Interestingly, high-energy γ -rays (100 MeV - 100 GeV) have been detected from some radio-loud NLS1s with *Fermi* Large Area Telescope (LAT; Abdo et al. 2009a,b; D’Ammando et al. 2012). The γ -ray detection implies the presence of relativistic jets in these objects, in direct analogy to blazars. To fully understand the cosmological evolution of supermassive BHs, it is therefore important to clarify the jet production efficiency and the jet duty cycle in such young systems in formation, or in other words to investigate in detail the radio-loud population of NLS1s.

In this Letter, we report our serendipitous discovery of dramatic optical variability in a peculiar radio-loud NLS1 candidate SDSS J110006.07+442144.3 (SDSS J1100+4421) by the Kiso Supernova Survey (KISS, Morokuma et al. 2014). Throughout this paper, we assume cosmological parameters $\Omega_\Lambda = 0.7$, $\Omega_M = 0.3$, and $h = 0.7$.

2. OBSERVATIONS

2.1. Discovery

SDSS J1100+4421 was detected as a transient object by the high-cadence optical transient survey KISS

(Morokuma et al. 2014). KISS uses the 1.05m Kiso Schmidt telescope equipped with Kiso Wide Field Camera (KWFC, Sako et al. 2012), which has a 2.2×2.2 deg field of view. In order to detect short-timescale transients, KISS adopts a 1 hr cadence; i.e., the same fields are repeatedly observed every 1 hr. The survey is performed with the optical g -band filter to detect shock breakout of supernovae (Tominaga et al. 2011; Morokuma et al. 2014).

Variability of SDSS J1100+4421 was first recognized on 2014 Feb 23.46 UT with $g = 19.73 \pm 0.13$ mag (Figure 1 and Table 1) and registered as a supernova candidate “KISS14k”. No source was present at this position in the stacked images taken 1 day before with a $5\text{-}\sigma$ limiting magnitude of 21.03 mag. Therefore this transient brightened at least by a factor of 3 within 1 day (1.3 mag day^{-1}). The SDSS images taken in 2003 show a faint object classified as a galaxy at the same position with $g = 22.16 \pm 0.11$ mag without spectroscopic data. Compared with the 2003 data, the 2014 flux increase is a factor of about 10. Hereafter we call this event a “flare”. This object is also recorded in USNO-B1.0 (Monet et al. 2003) and in the Guide Star Catalog II (GSC-II, Lasker et al. 2008) with variable magnitudes (Table 1).

After the flare, the brightness of SDSS J1100+4421 quickly declined in subsequent days. The stacked images show the fading object with about $g = 21.1$ and 21.5 mag on 2014 Feb 24 and 25, respectively. The decline rate during the first day after the flare is $0.9 - 1.3 \text{ mag day}^{-1}$.

2.2. Follow-up Observations

Immediately after the discovery (19.4 hr after the first detection), we started follow-up imaging and spectroscopic observations with the 8.2m Subaru telescope equipped with the Faint Object Camera And Spectrograph (FOCAS, Kashikawa et al. 2002). We took images and spectra of SDSS J1100+4421 three times during the same night. Typical seeing during the observations was $0''.5\text{--}0''.6$. Imaging data clearly show intranight variability.

Spectroscopic observations were performed using an offset $1.0''$ slit with the 300B grism and SY47 order-sorting filter³⁰. The spectral resolution is $\lambda/\Delta\lambda = 400$ (FWHM), which corresponds to a velocity resolution of 750 km s^{-1} . The obtained flux is consistent at a level of about 10% with the FOCAS photometry.

Figure 2 shows the optical spectra of SDSS J1100+4421. Emission lines of Mg II, [Ne V], [O II], [Ne III], H γ , H β , and [O III] are clearly identified, confirming the AGN nature of this object. All the emission lines consistently indicate a redshift of $z = 0.840$. All three spectra show a broad Mg II line with a FWHM of $2,070 \pm 100 \text{ km s}^{-1}$, which does not change with time. Although the H β line is dominated by the narrow component, the broad component is visible in the stacked spectrum (bottom panel of Figure 2). The FWHM of the broad H β is $1900 \pm 300 \text{ km s}^{-1}$. The widths of all the other narrow emission lines are not resolved with our spectra.

³⁰ This configuration gives clean 1st-order spectra in 4700–9000Å. Contamination of the 2nd-order spectrum exists at >9000 Å and it is estimated to be about 5% at 9200 Å for the spectra of SDSS J1100+4421.

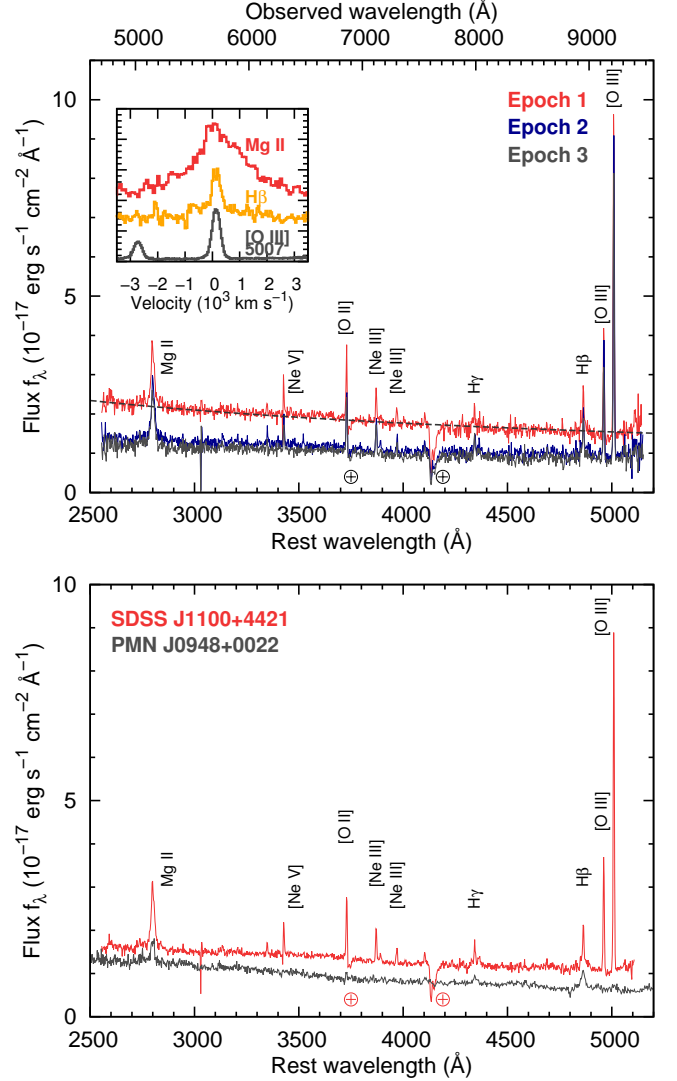


FIG. 2.— *Upper:* Optical spectra of SDSS J1100+4421 taken with Subaru/FOCAS on 2014 Feb 24 UT. Epochs 1, 2, and 3 correspond to MJD = 56712.29, 56712.55, and 56712.64, respectively. All the spectra are shown with 3 pixel binning (4.2 Å per binned pixel). The dashed line shows a power law fit with $f_\lambda \propto \lambda^{-0.6}$. Profiles of strong emission lines in the stacked spectrum are shown in the inset (in the original pixel scale). *Lower:* Stacked spectrum of SDSS J1100+4421 (3 pixel binning) compared with the SDSS spectrum of PMN J0948+0022 (flux scaled).

The continuum flux in the three spectra shows significant intranight variability. We find that the continuum of these spectra is well fitted by a power-law with a slope that is constant in time. The power-law index is $\alpha_\lambda = -0.60 \pm 0.01$ in all three epochs, where $f_\lambda \propto \lambda^{\alpha_\lambda}$, ($\alpha_\nu = -1.4$ for $f_\nu \propto \nu^{\alpha_\nu}$). In contrast to the continuum flux, the emission line fluxes in the three spectra are consistent within the uncertainty, e.g., the variation in the Mg II line flux is $\lesssim 10\%$. Emission line fluxes measured in the stacked spectrum are summarized in Table 1.

Optical and near infrared imaging follow-up observations were also performed with Horishima Optical and Near-Infrared camera (HONIR, Akitaya et al. 2014) of the 1.5m Kanata telescope, the Newtonian camera of the Kottamia Observatory 1.88m telescope, the

Kyoto Okayama Optical Low-dispersion Spectrograph (KOOLS) of the Okayama Astrophysical Observatory (OAO) 1.88m telescope (Yoshida 2005), and the 0.50m MITSuME telescope (Yatsu et al. 2007). Even after the flare, this object shows some variability (Figure 1), although the data are not densely sampled. The $r-i$ color during the flare (synthesized from the FOCAS spectra) is 0.25 mag, which is consistent with the SDSS $r-i$ color in 2003 (0.26 ± 0.21 mag).

In order to measure the X-ray flux of this object, Target of Opportunity (ToO) observations were performed with the Swift XRT (Burrows et al. 2005) on 2014 Mar 16-17 UT. An X-ray source was detected at a position consistent with SDSS J1100+4421. Assuming a power-law photon index of -2.0 (as for PMN J0948+0222, Abdo et al. 2009a), the average 0.3–8 keV flux reads as $(1.62 \pm 0.38) \times 10^{-13}$ erg s $^{-1}$ cm $^{-2}$.

3. DISCUSSION

3.1. Nature of SDSS J1100+4421

Our optical spectroscopy clearly indicates an AGN nature for SDSS J1100+4421. The relatively narrow widths of the broad Mg II and H β lines, FWHM $\lesssim 2000$ km s $^{-1}$, suggest in addition a NLS1 classification (e.g., Osterbrock & Pogge 1985; Pogge 2000; Komossa et al. 2006)³¹. However, SDSS J1100+4421 does not fit the other two characteristics of NLS1s, namely (i) the presence of Fe II bumps at 4400–4700 Å and 5150–5400 Å, and (ii) [O III]/H β flux ratio < 3 .

The absence of a Fe II bump may be naturally explained by a contribution from the additional prominent continuum component during the flare. This component can be interpreted as emission from a jet (Section 3.4). In fact, this object is found to be extremely radio loud (Section 3.2), and radio-loud AGNs tend to show weaker Fe II bumps (Boroson & Green 1992; Sulentic et al. 2003).

Figure 2 (bottom panel) shows that the spectrum of SDSS J1100+4421 is similar to that of NLS1 PMN J0948+0022 except for the narrow emission lines such as [O II] and [O III]. In fact, considering the properties of the broad emission lines and continuum, the narrow [O III] line is unusually strong, with the corresponding [O III]/H β flux ratio $\simeq 5 - 9$. Assuming a conventional conversion ($L_{5100} \simeq 10^{2.5} L_{[\text{O III}]}$ and $L_{\text{bol}} = 8.1 L_{5100}$, Shen et al. 2011; Runnoe et al. 2012), the [O III] line luminosity gives an estimate for the bolometric AGN luminosity $L_{\text{bol}} \simeq 8 \times 10^{45}$ erg s $^{-1}$. This is about 10 times higher than that estimated using the broad Mg II line, or the SDSS g -band flux in 2003, $L_{\text{bol}} = 5.2 L_{3000} \simeq 6 \times 10^{44}$ erg s $^{-1}$.

Based on these findings and considerations, we conclude that SDSS J1100+4421 is a candidate NLS1 with a particularly prominent power-law component and unusually strong narrow emission lines. Since the [O III] line strength is known to correlate with the radio power (e.g.,

³¹ Note that the dramatic optical variability observed, as well as the clearly detected broad components of the Mg II and H β lines, both invalidate a Seyfert 2 classification of SDSS J1100+4421. Also, the hardness ratio of the X-ray spectrum of the source, $(H - S)/(H + S) = -0.14 \pm 0.13$ (where H and S are the photon counts at < 2 keV and > 2 keV, respectively), does not indicate any heavy nuclear obscuration which could be expected for a type 2 AGN (Wang et al. 2004).

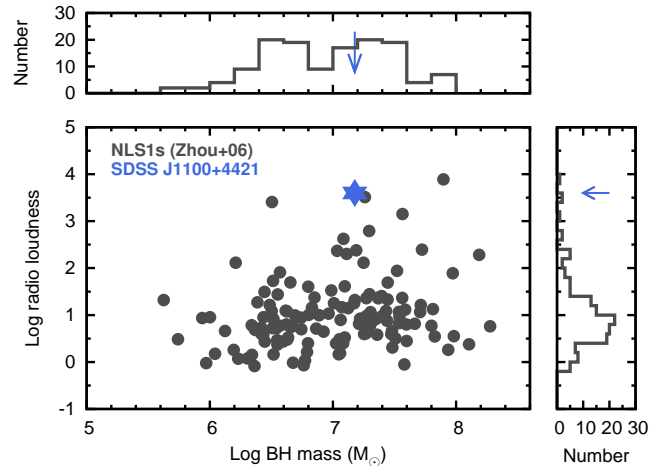


FIG. 3.— Radio loudness $R_{1.4}$ and BH mass for NLS1 samples from Z06 and for SDSS J1100+4421. The right and top panels show the histograms of radio loudness and BH mass, respectively. The values for SDSS J1100+4421 are shown with arrows.

Labiano 2008), the strong narrow components might be related to the extreme radio loudness and thus relativistic jets (Section 3.2).

3.2. Radio Properties

SDSS J1100+4421 is a strong radio source, which is recorded in various survey catalogs (Table 1). For a direct comparison with NLS1s, here we define a radio loudness parameter $R_{1.4}$ as in Z06, Komossa et al. (2006) and Yuan et al. (2008), i.e., as the ratio of f_ν (1.4 GHz) to f_ν (4400 Å) in the source rest frame (assuming radio and optical power-law slopes of $\alpha_\nu = -0.5$ for simple flux conversions).

Using the radio flux measured by FIRST and the SDSS g -band magnitude corrected for Galactic extinction ($A_V = 0.035$ mag, Schlegel et al. 1998), the radio loudness is $R_{1.4} \simeq 3 \times 10^3$. This is among the highest radio loudness values in the NLS1 samples (Figure 3). It should be noted that the epochs of various radio observations of SDSS J1100+4421 are not simultaneous with each other, or with those in other wavelengths; hence the evaluated radio loudness parameter is subject to an uncertainty generated by a source variability. However, even with the optical flux at the peak of the flare, the radio loudness is still very high, $R_{1.4} \simeq 4 \times 10^2$.

Interestingly, the radio structure in the FIRST image is extended compared with the beam size (Figure 1). The source has a core-dominated, two-sided structure with the linear size of 13'' (measured from the center to the north-west edge with 3σ flux level). This size corresponds to about 100 kpc (projected). If SDSS J1100+4421 is a NLS1, such a large-scale radio structure would be the largest known for this type of AGN (Doi et al. 2012, and references therein). Future high-resolution observations are needed to confirm the extension, and to investigate in detail the radio morphology of SDSS J1100+4421.

3.3. Black Hole Mass and Eddington Ratio

We estimate a mass of the BH in SDSS J1100+4421 with the following conventional method. Assuming the broad-line region (BLR) is virialized, the black hole mass

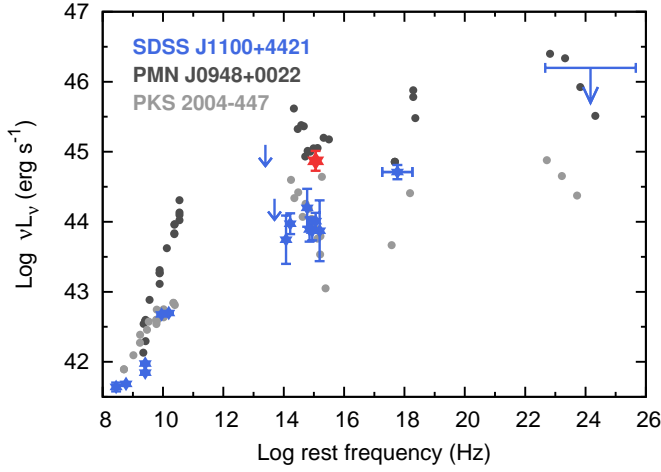


FIG. 4.— SED of SDSS J1100+4421 (blue) compared with that of γ -ray loud NLS1s PMN J0948+0022 (Abdo et al. 2009a) and PKS 2004-447 (Gallo et al. 2006; Abdo et al. 2009b). The optical flux of SDSS J1100+4421 during the flare is shown in red.

can be written as $M_{\text{BH}} = R_{\text{BLR}} v^2 / G$, where R_{BLR} is the size of BLR and $v = (\sqrt{3} \times \text{FWHM}/2)$ for an isotropic distribution of BLR clouds. The size of BLR (R_{BLR}) is known to correlate with the continuum and line luminosities (e.g., Kaspi et al. 2005). We use the empirical relations of McLure & Dunlop (2004, their Eqs A6 and A7), which give consistent BH mass estimates within 0.33 dex using $H\beta$ and Mg II . To avoid possible contamination from jet emission (Yuan et al. 2008), the continuum luminosities in the equations are replaced with the line luminosities by adopting the relations of Shen et al. (2011, L_{3000} and $L_{\text{Mg II}}$) and Greene & Ho (2005, L_{5100} and $L_{H\beta}$), respectively.

By adopting the luminosity and FWHM of the $H\beta$ and Mg II lines, we obtain $M_{\text{BH}} \sim 1.0 \times 10^7 M_{\odot}$ and $1.5 \times 10^7 M_{\odot}$, respectively. Given the higher S/N ratio, we adopt the estimate with the Mg II line in the following discussion. Figure 3 shows the radio loudness and BH mass compared with those of NLS1 samples by Z06. The BH masses for this sample are estimated using the luminosity and FWHM of the $H\beta$ line. The BH mass of SDSS J1100+4421 is within the distribution of BH masses of other NLS1s.

The bolometric luminosity of SDSS J1100+4421 is $L_{\text{bol}} \sim 6 \times 10^{44} \text{ erg s}^{-1}$ (Section 3.1), which is about 30 % of the Eddington luminosity ($L_{\text{Edd}} \sim 2 \times 10^{45} \text{ erg s}^{-1}$). Since radiative efficiency of the accretion disk at high (close to Eddington) accretion rates is of the order of 10%, the accretion luminosity of SDSS J1100+4421 is approximately $L_{\text{acc}} \sim 6 \times 10^{45} \text{ erg s}^{-1}$, corresponding to the mass accretion rate of $\dot{M}_{\text{acc}} = L_{\text{acc}}/c^2 \simeq 0.1 M_{\odot} \text{ yr}^{-1}$. The jet power estimated from the radio luminosity ($L_{1.4} = 7 \times 10^{43} \text{ erg s}^{-1}$) is $L_{\text{jet}} \sim 1 \times 10^{45} \text{ erg s}^{-1}$ (Cavagnolo et al. 2010), which confirms the high jet production efficiency.

3.4. Origin of the Flare

The long-term light curve rejects the flare in SDSS J1100+4421 as a transient phenomena, such as supernova or tidal disruption of a star. One might suppose that the flare arises from the variability of an accretion

disk, but that is also unlikely. Assuming a standard (optically thick, geometrically thin) disk structure around a BH with $M_{\text{BH}} \sim 1.5 \times 10^7 M_{\odot}$, the disk radius at which the bulk of the optical/ultraviolet emission is produced can be estimated as $R \sim 10^{15} \text{ cm} \sim 200 R_{\text{S}}$, where R_{S} is the Schwarzschild radius. This emitting radius is not changed significantly even for a super-critical, slim disk as long as $R > 10 R_{\text{S}}$ (e.g., Mineshige et al. 2000). The dynamical timescale at such a distance is a few tens of days, which is much longer than the observed timescale.

The remaining possibility for the origin of the flare is synchrotron emission from a relativistic jet. The presence of a jet is implied by the extreme radio loudness of the source. The steep slope of the optical spectra during the flare ($\alpha_{\nu} = -1.4$) is also consistent with synchrotron emission. Moreover, the observed variability timescale points out to the jet origin of the flare as well.

Optical variability on timescales shorter than a few days has been observed in other NLS1s (e.g., Klimek et al. 2004; Liu et al. 2010; Paliya et al. 2013; Maune et al. 2013; Eggen et al. 2013; Itoh et al. 2013). During the flare analyzed here, SDSS J1100+4421 brightens by a factor of at least 3 within about half a day in the rest frame. To our knowledge, such an extreme, blazar-like variability of a NLS1 has been confirmed for only γ -ray loud NLS1s (Liu et al. 2010; Maune et al. 2013; Eggen et al. 2013; Itoh et al. 2013).

Motivated by these similarities, the SED of SDSS J1100+4421 is compared with γ -ray loud NLS1s PMN J0948+0022 and PKS 2004-447 (Abdo et al. 2009a,b) in Figure 4. SDSS J1100+4421 is not detected in the Two Year Fermi-LAT catalog (2FGL, Nolan et al. 2012). If the γ -ray photon index is assumed to be -2.5 , in the analogy to PMN J0948+0022, the upper limit for the flux is $\sim 5 \times 10^{-12} \text{ erg s}^{-1} \text{ cm}^{-2}$. There is a large variety in the γ -ray loudness of the LAT-detected NLS1s; the upper limit for the γ -ray luminosity of SDSS J1100+4421 derived here is very close to the observed γ -ray luminosity of PMN J0948+0022, but it is higher than the luminosity of PKS 2004-447 by a factor of about 30.

4. SUMMARY

We report on the discovery of a dramatic optical variability from an enigmatic AGN, SDSS J1100+4421. This object seems like a NLS1 but is peculiar for its strong narrow emission lines and the large ($\sim 100 \text{ kpc}$) extent of the radio structure. The observational facts presented here suggest that this object has a young BH growing with an accretion rate close to the Eddington limit, and that the relativistic jets are efficiently produced and have evolved to the large scale. The dramatic optical variability, as well as the unusually strong narrow emission lines, are likely to be produced by the relativistic jets. Our discovery demonstrates that high-cadence surveys are potentially useful to search for such a rare class of AGNs and to study the jet production/duty cycle in the growing BHs.

We thank the OAO staff for continuous support and the *Swift* team for approving our ToO request and performing the observations. This research is based in part on data collected at Subaru Telescope, which is operated by the National Astronomical Observatory of Japan.

This research has made use of the NASA/IPAC Extragalactic Database (NED) which is operated by the Jet Propulsion Laboratory, California Institute of Technology, under contract with the National Aeronautics and Space Administration. The National Radio Astronomy Observatory is a facility of the National Science Foundation operated under cooperative agreement by Associ-

ated Universities, Inc. This research has been supported by the Grant-in-Aid for Scientific Research (23740143, 23740157, 24740117, 25103515, 25800103) of the Japan Society for the Promotion of Science (JSPS) and of the Ministry of Education, Culture, Sports, Science and Technology (MEXT) and by INAF PRIN 2011 and PRIN MIUR 2010/2011.

REFERENCES

- Abdo, A. A., et al. 2009a, *ApJ*, 699, 976
 —. 2009b, *ApJ*, 707, L142
 Akitaya, H., et al. 2014, *Proc. SPIE*, 9147, 91474O
 Boroson, T. A., & Green, R. F. 1992, *ApJS*, 80, 109
 Burrows, D. N., et al. 2005, *Space Sci. Rev.*, 120, 165
 Caccianiga, A., et al. 2014, *MNRAS*, 441, 172
 Cavagnolo, K. W., McNamara, B. R., Nulsen, P. E. J., Carilli, C. L., Jones, C., & Birzan, L. 2010, *ApJ*, 720, 1066
 Condon, J. J., Cotton, W. D., Greisen, E. W., Yin, Q. F., Perley, R. A., Taylor, G. B., & Broderick, J. J. 1998, *AJ*, 115, 1693
 D’Ammando, F., et al. 2012, *MNRAS*, 426, 317
 Doi, A., Nagira, H., Kawakatu, N., Kino, M., Nagai, H., & Asada, K. 2012, *ApJ*, 760, 41
 Eggen, J. R., Miller, H. R., & Maune, J. D. 2013, *ApJ*, 773, 85
 Gallo, L. C., et al. 2006, *MNRAS*, 370, 245
 Greene, J. E., & Ho, L. C. 2005, *ApJ*, 630, 122
 Gregory, P. C., Scott, W. K., Douglas, K., & Condon, J. J. 1996, *ApJS*, 103, 427
 Hales, S. E. G., Riley, J. M., Waldram, E. M., Warner, P. J., & Baldwin, J. E. 2007, *MNRAS*, 382, 1639
 Itoh, R., et al. 2013, *ApJ*, 775, L26
 Kashikawa, N., et al. 2002, *PASJ*, 54, 819
 Kaspi, S., Maoz, D., Netzer, H., Peterson, B. M., Vestergaard, M., & Jannuzi, B. T. 2005, *ApJ*, 629, 61
 Klimek, E. S., Gaskell, C. M., & Hedrick, C. H. 2004, *ApJ*, 609, 69
 Komossa, S., Voges, W., Xu, D., Mathur, S., Adorf, H.-M., Lemson, G., Duschl, W. J., & Grupe, D. 2006, *AJ*, 132, 531
 Labiano, A. 2008, *A&A*, 488, L59
 Lasker, B. M., et al. 2008, *AJ*, 136, 735
 Liu, H., Wang, J., Mao, Y., & Wei, J. 2010, *ApJ*, 715, L113
 Mathur, S. 2000, *MNRAS*, 314, L17
 Maune, J. D., Miller, H. R., & Eggen, J. R. 2013, *ApJ*, 762, 124
 McLure, R. J., & Dunlop, J. S. 2004, *MNRAS*, 352, 1390
 Mineshige, S., Kawaguchi, T., Takeuchi, M., & Hayashida, K. 2000, *PASJ*, 52, 499
 Monet, D. G., et al. 2003, *AJ*, 125, 984
 Morokuma, T., et al. 2014, *PASJ*, in press
 Myers, S. T., et al. 2003, *MNRAS*, 341, 1
 Nolan, P. L., et al. 2012, *ApJS*, 199, 31
 Osterbrock, D. E., & Pogge, R. W. 1985, *ApJ*, 297, 166
 Paliya, V. S., Stalin, C. S., Kumar, B., Kumar, B., Bhatt, V. K., Pandey, S. B., & Yadav, R. K. S. 2013, *MNRAS*, 428, 2450
 Pogge, R. W. 2000, *New A Rev.*, 44, 381
 Rengelink, R. B., Tang, Y., de Bruyn, A. G., Miley, G. K., Bremer, M. N., Roettgering, H. J. A., & Bremer, M. A. R. 1997, *A&AS*, 124, 259
 Runnoe, J. C., Brotherton, M. S., & Shang, Z. 2012, *MNRAS*, 422, 478
 Sako, S., et al. 2012, *Proc. SPIE*, 8446, 84466L
 Schlegel, D. J., Finkbeiner, D. P., & Davis, M. 1998, *ApJ*, 500, 525
 Shen, Y., et al. 2011, *ApJS*, 194, 45
 Sikora, M., Stawarz, L., & Lasota, J.-P. 2007, *ApJ*, 658, 815
 Sulentic, J. W., Zamfir, S., Marziani, P., Bachev, R., Calvani, M., & Dultzin-Hacyan, D. 2003, *ApJ*, 597, L17
 Tominaga, N., Morokuma, T., Blinnikov, S. I., Baklanov, P., Sorokina, E. I., & Nomoto, K. 2011, *ApJS*, 193, 20
 Wang, J. X., Malhotra, S., Rhoads, J. E., & Norman, C. A. 2004, *ApJ*, 612, L109
 Whalen, D. J., Laurent-Muehleisen, S. A., Moran, E. C., & Becker, R. H. 2006, *AJ*, 131, 1948
 White, R. L., Becker, R. H., Helfand, D. J., & Gregg, M. D. 1997, *ApJ*, 475, 479
 Yatsu, Y., et al. 2007, *Physica E Low-Dimensional Systems and Nanostructures*, 40, 434
 Yoshida, M. 2005, *Journal of Korean Astronomical Society*, 38, 117
 Yuan, W., Zhou, H. Y., Komossa, S., Dong, X. B., Wang, T. G., Lu, H. L., & Bai, J. M. 2008, *ApJ*, 685, 801
 Zhou, H., Wang, T., Yuan, W., Lu, H., Dong, X., Wang, J., & Lu, Y. 2006, *ApJS*, 166, 128

TABLE 1
SUMMARY OF NEW AND ARCHIVAL DATA FOR SDSS J1100+4421

MJD ^a	UT ^a	Filter	Magnitude ^b	Exp. time (sec)	Telescope ^c
56325.66	2013 Feb 02	<i>g</i>	>20.65 ^d	180 × 5	1
56709.50	2014 Feb 21	<i>g</i>	>20.77 ^d	180 × 5	1
56710.51	2014 Feb 22	<i>g</i>	>21.03 ^d	180 × 5	1
56711.46	2014 Feb 23	<i>g</i>	19.73 ± 0.13	180	1
56711.51	2014 Feb 23	<i>g</i>	20.22 ± 0.17	180	1
56711.55	2014 Feb 23	<i>g</i>	19.96 ± 0.11	180	1
56711.60	2014 Feb 23	<i>g</i>	19.82 ± 0.10	180	1
56712.72	2014 Feb 24	<i>g</i>	21.08 ± 0.10	180 × 41	1
56713.63	2014 Feb 25	<i>g</i>	21.50 ± 0.10	180 × 44	1
56718.65	2014 Mar 02	<i>g</i>	>20.52 ^d	180 × 8	1
56726.51	2014 Mar 10	<i>g</i>	>19.78 ^d	60 × 27	2
56727.56	2014 Mar 11	<i>g</i>	>20.00 ^d	180 × 36	1
56731.53	2014 Mar 15	<i>g</i>	19.87 ± 0.51	60 × 26	2
56732.53	2014 Mar 16	<i>g</i>	>19.39 ^d	60 × 54	2
56738.73	2014 Mar 22	<i>g</i>	>20.49 ^d	180 × 4	1
56739.73	2014 Mar 23	<i>g</i>	>20.37 ^d	180 × 5	1
56747.65	2014 Mar 31	<i>g</i>	21.50 ± 0.30	180 × 13	3
56749.47	2014 Apr 02	<i>g</i>	21.70 ± 0.30	180 × 6	3
56712.63	2014 Feb 24	<i>i</i>	20.72 ± 0.01	30	4
56712.27	2014 Feb 24	<i>B</i>	21.17 ± 0.02	25	4
56712.55	2014 Feb 24	<i>B</i>	21.72 ± 0.02	15	4
56712.63	2014 Feb 24	<i>B</i>	21.78 ± 0.02	30	4
56726.93	2014 Mar 10	<i>V</i>	19.17 ± 0.08	300 × 4	5
56712.62	2014 Feb 24	<i>R_c</i>	20.48 ± 0.12	140 × 5	6
56726.51	2014 Mar 10	<i>R_c</i>	19.48 ± 0.19	60 × 27	2
56726.75	2014 Mar 10	<i>R_c</i>	19.73 ± 0.06	140 × 7	6
56726.93	2014 Mar 10	<i>R_c</i>	20.01 ± 0.10	300 × 4	5
56731.53	2014 Mar 15	<i>R_c</i>	19.58 ± 0.46	60 × 26	2
56732.53	2014 Mar 16	<i>R_c</i>	19.48 ± 0.39	60 × 54	2
56726.51	2014 Mar 10	<i>I_c</i>	18.89 ± 0.48	60 × 27	2
56726.77	2014 Mar 10	<i>I_c</i>	19.41 ± 0.10	140 × 7	6
56731.53	2014 Mar 15	<i>I_c</i>	18.50 ± 0.20	60 × 26	2
56732.53	2014 Mar 16	<i>I_c</i>	18.91 ± 0.19	60 × 54	2
56712.60	2014 Feb 24	<i>J</i>	18.74 ± 0.60	120 × 5	6
56726.75	2014 Mar 10	<i>J</i>	18.10 ± 0.11	120 × 7	6
56732.68	2014 Mar 16	<i>J</i>	17.43 ± 0.07	120 × 9	6
56733.61	2014 Mar 17	<i>J</i>	17.72 ± 0.11	120 × 12	6
56726.77	2014 Mar 10	<i>K_s</i>	16.01 ± 0.07	120 × 7	6
56732.70	2014 Mar 16	<i>K_s</i>	15.84 ± 0.08	120 × 9	6
	UT	Filter	Magnitude	Source	Offset ^e
	1966	<i>B</i>	20.09	USNO-B1.0	0.6''
	1966	<i>B</i>	20.58	USNO-B1.0	0.6''
	1994	<i>B_j</i>	22.06 ± 0.65	GSC-II	0.3''
	1994	<i>B</i>	20.73 ± 0.51	GSC-II	0.3''
	2003 Mar 24	<i>u</i>	22.76 ± 0.40	SDSS	
		<i>g</i>	22.16 ± 0.11	SDSS	
		<i>r</i>	22.17 ± 0.13	SDSS	
		<i>i</i>	21.91 ± 0.16	SDSS	
		<i>z</i>	20.94 ± 0.25	SDSS	
	2010	<i>W1</i>	17.41 ± 0.14	WISE	0.36''
		<i>W2</i>	16.93 ± 0.32	WISE	0.36''
		<i>W3</i>	> 12.78 ^f	WISE	0.36''
		<i>W4</i>	> 8.63 ^f	WISE	0.36''
	UT	Frequency (GHz)	Flux (mJy)	Source ^g	Offset ^e
	1976-1978	0.151	91 ± 13	7C	0.11'
	1991-1996	0.325	47	WENSS	0.46'
	1993-1997	1.4	21.3 ± 0.8	NVSS	0.04'
	1995-1998	1.4	15.76 ± 0.13	FIRST	0.003'
	1986-1987	4.85	31 ± 4	GB6	0.047'
	1995 Aug 14	8.4	18.8	CLASS	0.004'

TABLE 1
CONTINUED

Line	Flux (10^{-17} erg s $^{-1}$ cm $^{-2}$)	Luminosity (10^{41} erg s $^{-1}$)
Mg II 2798	48.9 ± 2.8	15.6 ± 0.9
[Ne V] 3425	7.7 ± 0.7	2.5 ± 0.2
[O II] 3727	17.0 ± 1.6	5.4 ± 0.5
[Ne III] 3869	10.2 ± 0.3	3.3 ± 0.1
[Ne III] 3968	5.2 ± 0.7	1.7 ± 0.2
H γ (narrow)	5.8 ± 0.6	1.9 ± 0.2
H β (narrow)	10.3 ± 1.8	3.3 ± 0.6
H β (broad)	16.2 ± 2.7	5.2 ± 0.9
[O III] 4959	30.9 ± 1.0	9.9 ± 0.3
[O III] 5007	93.5 ± 1.4	29.9 ± 0.4

NOTE. — ^a Average time for stacked data. ^b AB magnitudes for SDSS *ugriz* filters and Vega magnitudes for the other filters. ^c 1. Kiso/KWFC, 2. MITSuME, 3. OAO/KOOLS, 4. Subaru/FOCAS, 5. Kottamia Observatory, 6. Kanata/HONIR ^d 5σ upper limit. ^e Offset from the source position in the SDSS images. ^f 95 % confidence upper limit in AllWISE Source Catalog. ^g The survey/catalog abbreviations and references: Seventh Cambridge Survey (7C, Hales et al. 2007), Westerbork Northern Sky Survey (WENSS, Rengelink et al. 1997), Faint Images of the Radio Sky at Twenty-Centimeters (FIRST, White et al. 1997), NRAO VLA Sky Survey (NVSS, Condon et al. 1998), Green Bank 6-cm Radio Source Catalog (GB6, Gregory et al. 1996), The Cosmic Lens All-Sky Survey (CLASS, Myers et al. 2003).